



Contents lists available at ScienceDirect

Electronic Journal of Biotechnology

journal homepage:

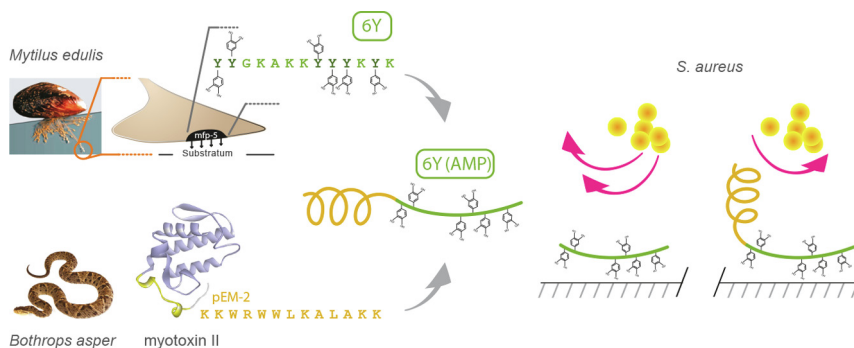


Research Article

Antimicrobial characterization of a titanium coating derived from mussel-glue and *Bothrops asper* snake venom for the prevention of implant-associated infections caused by *Staphylococcus* ☆

Adriana Gauna^{a,*}, Luis Mercado^b, Fanny Guzmán^c^a Doctorado en Biotecnología, Pontificia Universidad Católica de Valparaíso-Universidad Técnica Federico Santa María, Avenida Universidad n°330, Curauma, Valparaíso, Chile^b Instituto de Biología, Pontificia Universidad Católica de Valparaíso, Avenida Universidad n°330, Curauma, Valparaíso, Chile^c Núcleo de Biotecnología Curauma, Pontificia Universidad Católica de Valparaíso, Avenida Universidad n°330, Curauma, Valparaíso, Chile

GRAPHICAL ABSTRACT



ARTICLE INFO

Article history:

Received 19 September 2021

Accepted 1 February 2022

Available online 7 February 2022

Keywords:

Antifouling coating
 Antimicrobial peptides
 Bothrops asper snake venom
 Implant-associated infection
 Mussel coating
 Mussel-glue
 Orthopedic implants
 Staphylococcus aureus
 Staphylococcus epidermidis
 Staphylococcus infection
 Titanium coating

ABSTRACT

Background: Proliferation of bacteria, such as *Staphylococcus aureus* and *Staphylococcus epidermidis*, on orthopedic implants has been a challenge in orthopedic surgery, highlighting the problem of the increasing antibiotic resistance and the necessity to develop new antimicrobial agents. In this sense, antimicrobial peptides are promising candidates, which can be attached to titanium surfaces in order to make them safer. *Mytilus* mussels are characterized by adhering efficiently to a wide variety of surfaces, especially metallic ones, through adhesive proteins with a high content of dihydroxyphenylalanine, which is a post-translational modification of tyrosine.

Results: This work refers to the synthesis of a coating based on a bifunctional peptide that combines a sequence derived from the mussel foot protein-5 and the antimicrobial peptide pEM-2, derived from *Bothrops asper* snake venom. The adhesive properties of this bifunctional peptide were evaluated, as well as the adhesive sequence without the pEM-2, using a Quartz Crystal Microbalance. The results showed that the presence of the antimicrobial peptide improved the adhesion; however, a loss of the bactericidal activity was observed. Even so, the adhesive sequence by itself exhibited an important antifouling activity, preventing *S. aureus* and *S. epidermidis* adhesion to titanium by 75% and 45%, respectively, although the result against *S. epidermidis* was not significant.

Conclusions: A 13-residue peptide derived from a natural and biocompatible source, like a *Mytilus* mussel adhesive protein, could be projected as a protective agent on titanium surfaces against *S. aureus* and

Peer review under responsibility of Pontificia Universidad Católica de Valparaíso

* Corresponding author.

E-mail address: adriana.gauna.s@mail.pucv.cl (A. Gauna).<https://doi.org/10.1016/j.ejbt.2022.02.001>

0717-3458/© 2022 Universidad Católica de Valparaíso. Production and hosting by Elsevier B.V.

This is an open access article under the CC BY-NC-ND license (<http://creativecommons.org/licenses/by-nc-nd/4.0/>).

S. epidermidis, being responsible for two thirds of the cases of orthopedic implant infection.

How to cite: Gauna A, Mercado L, Guzmán F. Antimicrobial characterization of a titanium coating derived from mussel-glue and *Bothrops asper* snake venom for the prevention of implant-associated infections caused by *Staphylococcus*. Electron J Biotechnol 2022;56. <https://doi.org/10.1016/j.ejbt.2022.02.001>.

© 2022 Universidad Católica de Valparaíso. Production and hosting by Elsevier B.V. This is an open access article under the CC BY-NC-ND license (<http://creativecommons.org/licenses/by-nc-nd/4.0/>).

1. Introduction

Infections are a significant problem in orthopedic surgery that often leads to implant failure and replacement and, in severe cases, can result in amputation and even mortality [1]. Most of implant-associated infections are caused by gram-positive *Staphylococcus* bacteria [2].

Several strategies have been adopted in order to reduce the risk of infection; some of them included the adhesion of functional coatings. The first approach to these coatings is to prevent infection by preparing the surface to hinder microbial colonization. Then, there are coatings whose function is not to prevent microbial adhesion, but to kill those microorganisms that do adhere [3]. This latter category includes coatings based on antimicrobial peptides, which are immobilized on surfaces using different techniques [4,5,6].

Antimicrobial peptides (AMP) are attractive candidates as therapeutic agents because they are capable of killing a broad spectrum of bacteria (including typically multi-resistant strains), fungi, and viruses by a non-specific membranolytic mechanism, reducing the development of antimicrobial resistance [7,8]. AMP are small peptides (from 12 to 80 amino acids, corresponding to molecular weight from 1 to 5 kDa), mostly cationic and amphipathic [9]. These characteristics allow most of them to bind to the negatively charged bacterial cell membrane of bacteria via electrostatic interactions, leading to cell disruption and rapid death, while other peptides act indirectly by modulating the host defense system [10,11].

PEM-2 (KKWRWWLKALAKK) is an AMP derived from myotoxin II, a phospholipase A2 homolog, present in the *Bothrops asper* snake venom. This peptide showed high bactericidal activity against *Salmonella typhimurium* and *Staphylococcus aureus* strains, with low toxicity to muscle cells [12]. In subsequent studies, the pEM-2 peptide was shown to have fungicidal properties against a variety of *Candida* species, killing 100% of the yeast cells at concentrations close to 5 μ M, an activity that is partially inhibited by high concentrations of extracellular divalent cations (Ca^{2+} or Mg^{2+}), in accordance to its proposed mechanism of action as a membrane permeabilizer [13].

Mytilus mussels are known for their ability to adhere to marine surfaces by the secretion of adhesive proteins that form a solid plaque, capable of mediating firm attachment to a wide variety of wet surfaces, such as rocks, metal, polymer and wood structures. The adhesive and cohesive properties of mussel foot proteins (Mfps) have been linked to the presence of L-3,4-dihydroxyphenylalanine (DOPA), a catecholic amino acid that is formed by post-translational modification of tyrosine [14]. These DOPA residues confer these adhesives a great versatility due to their ability to form hydrogen bonds with hydrophilic surfaces and participate in coordination bonds with ions and metal oxides. Six Mfps have been described, where Mfp-5 is recognized as the main adhesive protein with the higher DOPA content (28%) and a mass of 9 kDa [15,16].

Some works have explored the adhesive properties of DOPA residues in the development of new coatings based on synthetic peptides, which are functionalized with chemical groups or polymers with antifouling properties [17,18,19]. Other investigators have expressed some fusion proteins in *E. coli* cells based on the

sequence of mussel adhesive proteins and peptide sequences with silver-binding [20] or osseointegration [21] properties to be used in medical materials to increase their biocompatibility and safety.

Inspired by the versatility and biocompatibility of mussel adhesion, we synthesized a novel bifunctional peptide that combines a sequence derived from Mfp-5 and the antimicrobial sequence of pEM-2 in order to obtain a coating for the prevention of implant-associated infections.

2. Materials and methods

2.1. Peptide selection and synthesis

13-Mer adhesive peptide with a high content of DOPA and Lys residues was selected from FASTA sequence of *Mytilus edulis* Mfp-5 (GenBank accession no. AAL35297.1). This peptide was synthesized with and without the antimicrobial peptide pEM-2 (Table 1) using standard Fmoc chemistry on Rink amide resin (0.55 meq/g) using N,N,N',N'-tetramethyl-O-(1H-benzotriazol-1-yl)uronium hexafluorophosphate (HBTU) and O-(1H-6-chlorobenzotriazole-1-yl)-1,1,3,3-tetramethyluronium hexafluorophosphate (HCTU) as activators and *in situ* neutralization with ethyldiisopropylamine (DIPEA) in N,N-dimethylformamide (DMF) as solvent. Fmoc deprotection was carried out using a solution of 20% of 4-methylpiperidine in DMF. Peptides were cleaved using a solution of trifluoroacetic acid/triisopropylsilane/2,2'-(ethylenedioxy)diethanethiol/water (92.5/2.5/2.5/2.5) and purified by RP-HPLC to a purity higher than 90% [22,23]. The molecular mass and purity of peptides were confirmed by electrospray ionization mass spectrometry (Shimadzu Corp., Kyoto, Japan) and RP-HPLC, respectively.

2.2. Incorporation of DOPA by enzymatic hydroxylation

At this point the sequences were synthesized with tyrosine residues and an enzymatic treatment was necessary to obtain the adhesive or modified versions of the sequences. Tyr residues in the peptides were then hydroxylated to DOPA using a commercially available mushroom tyrosinase (Sigma-Aldrich). Reaction buffer was made by dissolving 0.1 M Na_2HPO_4 and 50×10^{-3} M $\text{Na}_2\text{B}_4\text{O}_7$ in water, with ascorbic acid subsequently added to adjust the pH to 7.0. 4 mg of peptides was first dissolved in 2 mL of water and then 8 mL of reaction buffer was added to obtain the final peptide solution, which turned cloudy at that point. 1 mg of mushroom tyrosinase was dissolved in 0.2 mL buffer and added to the peptide solution and the resulting mixture was constantly stirred for 2 h at room temperature. Finally, 0.5 mL of glacial acetic acid was added to stop the reaction. Modified peptides were purified by RP-HPLC and the molecular mass was confirmed by MALDI

Table 1
Synthetic adhesive and bifunctional peptides derived from Mfp-5 and pEM-2 sequences. DOPA residues are denoted as Y*.

Internal ID	Sequence
6Y(AMP)	KKWRWWLKALAKKY*Y*GKAKKY*Y*Y*KY*K
6Y	Y*Y*GKAKKY*Y*Y*KY*K

mass spectrometry. Peptides were stored as lyophilized powders at room temperature and dissolved just before use [24].

2.3. Quartz crystal microbalance (QCM) measurements

QCM-D (QSense® Analyzer) measurements were carried out with titanium probes, studying the deposition and coating stability of the peptides. Solutions of 1 mg/mL of peptides were prepared in 0.1 M acetate buffer pH 3. Subsequent washing steps were done with the same buffer solution of deposition. Data were processed using QSense Dfind software (Biolin Scientific) [25].

Graphics and statistical calculations were performed by the Graphpad Prism v6.1 for Windows (GraphPad software, San Diego, CA, USA). Results were expressed as mean plus standard deviation. The results were analyzed by Tukey's two-way ANOVA multiple comparison test. Significant differences were determined at $P < 0.0001$.

2.4. Antimicrobial assays for pEM-2

Antibacterial activity of peptide pEM-2 was determined against *Staphylococcus aureus* (ATCC 25933) and *Staphylococcus epidermidis* (ATCC 35984). The minimum bactericidal concentration (MBC) was evaluated in 96-well microtiter plates as reported [26]. Bacteria were cultured overnight in trypticase soy broth (TSB) and diluted until reaching an optical density (OD_{600}) of 0.4–0.7. Cultures containing 1×10^7 colony-forming units per milliliter (CFU/mL) were exposed for 1 h at 37°C to peptide solutions of 10, 20 and 30 μ M. Following the exposure, bacteria were subjected to seven ten-fold serial dilutions and incubated for 16 h at 37°C in fresh TSB media. All assays were carried out in triplicate and surviving bacteria were quantified as colony-forming units per milliliter (CFU/mL) for each peptide concentration.

2.5. Circular dichroism (CD) spectroscopy

CD spectroscopy of each peptide, including bifunctional, adhesive and the pEM-2 peptides, was carried out on a JASCO J-815 CD spectrometer (JASCO Corp., Tokyo, Japan) in the far ultraviolet (UV) range (190–250 nm), using quartz cuvettes (0.1 cm path length). Each spectrum was recorded averaging three scans in continuous scanning mode. Solvent blank was subtracted from each sample spectrum. Molar ellipticity was calculated for each peptide using 250 μ L of 2 mM peptide in 30% (v/v) 2,2,2-trifluoroethanol. Resulting data were analyzed using Spectra Manager software (Version 2.0, JASCO Corp., Tokyo, Japan) [27].

2.6. Antimicrobial assays on substrate

1 cm-diameter titanium discs (grade 5) were used as substrates, which were previously washed once with a solution 2% dodecyl sodium sulfate (SDS) for 10 min and four times with ultrapure water and finally sonicated for 10 min in pure ethanol. Clean discs were modified overnight by peptide adsorption into the buffer solution mentioned above, gently washed with ultrapure water to remove the no-adhered peptide and dried.

Modified and unmodified substrates were placed in 24 well plates, UV-sterilized for 15 min and covered with 570 μ L of tryptic soy broth (TSB) medium. 30 μ L of 1×10^7 CFU/mL of *S. aureus* and *S. epidermidis* culture in exponential growth phase was added and incubated for 24 h at 37°C. Samples were rinsed using 250 μ L of phosphate-buffered saline (PBS) and three independent assays were conducted:

- (1) Substrates were treated with a Live/Dead Cell Double Staining kit (Sigma-Aldrich) and the image was capture using an epifluorescence Ti Nikon microscopy, provided with the NIS Elements software.
- (2) Bacteria were then detached from the substrates by immersion of the samples in PBS, agitation for 3 min using an ultrasonic bath, and vortex mixing for 1 min. 100 μ L of the resulting detachment solution were transferred to a 96-well microplate, and after adding 150 μ L of TBS to each well, optical density changes were measured at 600 nm during 24 h at 37°C [28].
- (3) Bacteria were fixed overnight in 500 μ L of 2.5% (v/v) glutaraldehyde in PBS at 4°C. Subsequently, the samples were dehydrated with graded ethanol and then dried. A small amount of platinum was sputtered on the samples to avoid charging in the microscope. Cells were examined under a scanning electron microscope (Hitachi SU 3500, Tokyo, Japan). This assay was accomplished just with the bifunctional peptide to observe the possible effect of the antimicrobial sequence adhered to Ti on *S. aureus* [29].

3. Results and discussion

3.1. Adhesion properties of synthetic peptides

An adhesive sequence derived from the Mfp-5 with six DOPA residues was selected to be synthesized as a unique lineal peptide together with the pEM-2 antimicrobial sequence in the N-terminus, due to the importance of the positive charge of the amine group in the antimicrobial activity. The adhesive sequence with only 13 residues was synthesized as well. The sequences are summarized in Table 1 and Fig. 1, when the internal ID denotes the number of DOPA residues and the presence of the antimicrobial peptide (AMP).

Peptide adhesion was determined using a quartz crystal microbalance (QCM) equipment in which the amount of material attached is recorded as a decrease in the frequency of the quartz resonator and, similarly, an increase in frequency denotes a material removal. So, this equipment, depending on the characteristics of the film, allows to calculate the amount of adhered material through a direct relationship with the frequency change in the resonator (Δf). Two factors were considered to determine their effect in the deposition and coating stability of synthetic peptides: the presence of antimicrobial sequence and the modification of tyrosine to DOPA.

We used the peptide 6Y(AMP) and its version without the antimicrobial sequence 6Y, in its modified and unmodified versions. Fig. 2 shows that the modified versions of both peptides (orange and green) not only showed a greater amount of material attached (higher Δf), but the adhesion was stable after 30 min of subsequent washing with the same deposition buffer. Unmodified peptides (blue and magenta) had a lower and unstable adhesion, as shown by the increasing frequency during washing, denoting a partial removal of the material.

On the other hand, the presence of the antimicrobial sequence pEM-2 favored the adhesion of the 6Y(AMP) versus the 6Y peptide. It can be thought that a higher Δf could be due to the considerably higher molecular mass of 6Y(AMP) and that is why the calculation for molar density was carried out using the Sauerbrey equation [30]. This equation can be used only when the coating is a rigid film and the change in resonator dissipation is less than 5% of the Δf , which proved to be true for all coatings reported in this work.

The data expressed as surface molar density (Fig. 3) allowed us to make a more realistic comparison of the different coatings and to determine that the presence of the antimicrobial peptide effectively enhances the adhesion, probably due to its high lysine

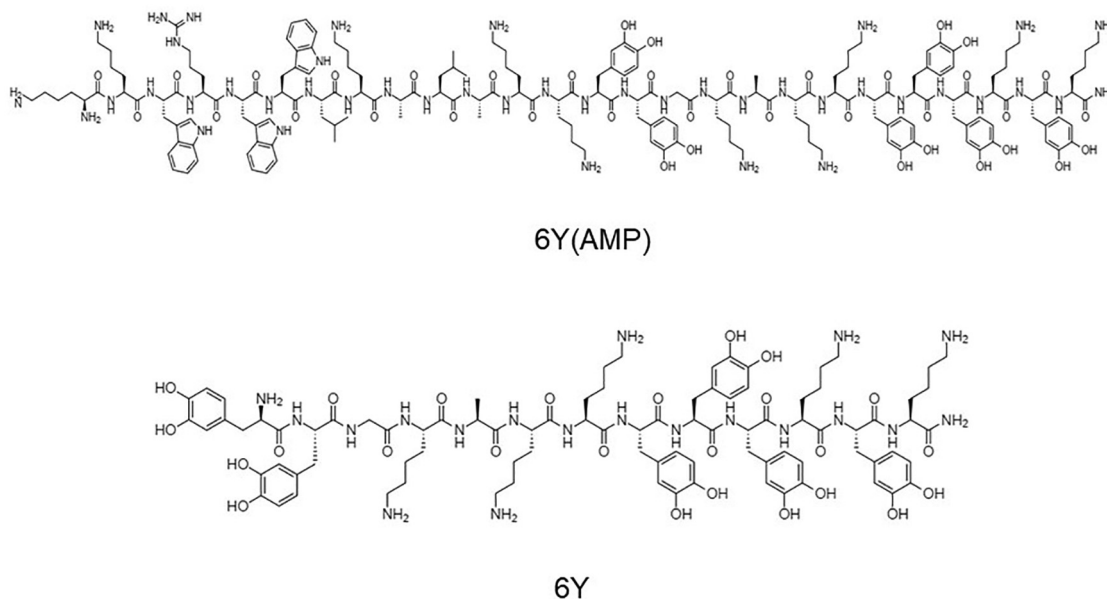


Fig. 1. Structure of peptides 6Y(AMP) and 6Y.

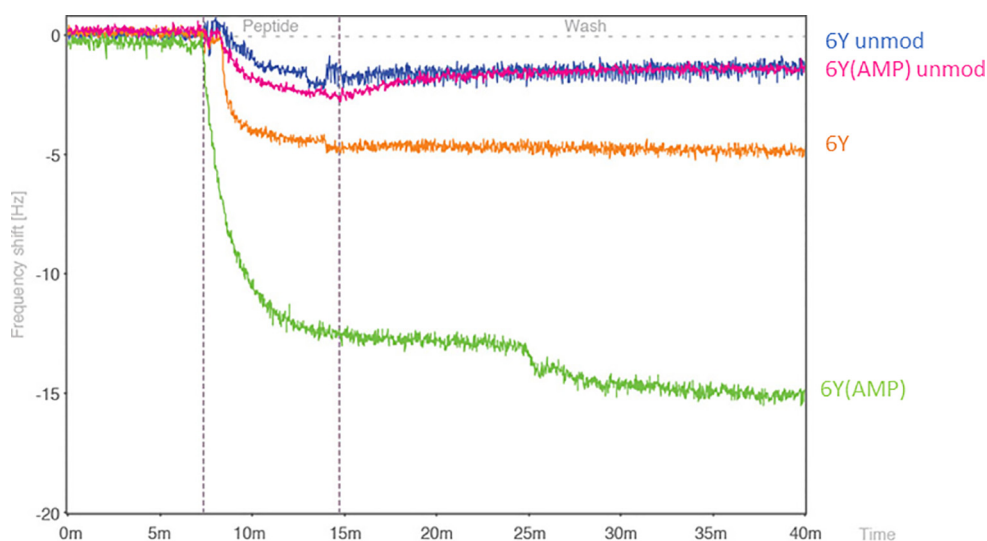


Fig. 2. QCM measurements of 6Y and 6Y(AMP) and their modified version. The enzymatic modification and the presence of AMP caused a higher frequency shift.

content, which favors it by three different mechanisms: 1) By displacing surface water and ions to increase the effective binding sites; 2) By being directly involved in cooperative surface binding in a sequence dependent manner; 3) By enhancing cohesion by Michael addition to oxidized species or by forming cation- π interactions [31]. Recently, Maier et al. [32] and others [33,34] utilized surface forces apparatus (SFA) to study the adaptive synergy between amine and catechol in binding to wet mica, using small molecule cyclic analogs with Lys or Arg present adjacent to catechol or phenyl groups. Their results showed that the adhesion energy is remarkably higher when both catechol and amine are present, suggesting a synergistic effect between these functional motifs.

3.2. Antimicrobial activity for pEM-2 and circular dichroism spectroscopy

Antibacterial activity of peptide pEM-2 was determined against *Staphylococcus aureus* (ATCC 25933) and *Staphylococcus epider-*

midis (ATCC 35984) and a minimum bactericidal concentration (MBC) of $10 \mu\text{M}$ was enough to kill the bacteria at a concentration of 1×10^7 CFU/mL. Due to the importance that the secondary structure has in the antimicrobial activity of this peptide, CD analyses of pEM-2, as well as bifunctional and adhesive peptides were carried out. These results are summarized in Fig. 4.

Circular dichroism results showed that the antimicrobial peptide pEM-2 has a α -helix structure, a structure that is very important in the antimicrobial activity, in agreement with ^1H NMR analysis accomplished by Yu et al. [35]. Therefore, it is crucial that the binding of this AMP to adhesive sequences does not affect its structure, so the antimicrobial activity could remain intact and may be transferred to the surface to be coated.

It should be noted that the adhesive sequence 6Y showed a random structure, but the bifunctional peptide 6Y(AMP) showed a α -helix structure, indicating that the presence of the adhesive sequence, with more random characteristics, does not affect significantly the structure of AMP. This indicates that the coating could well preserve and transfer the bactericidal properties of pEM-2 to

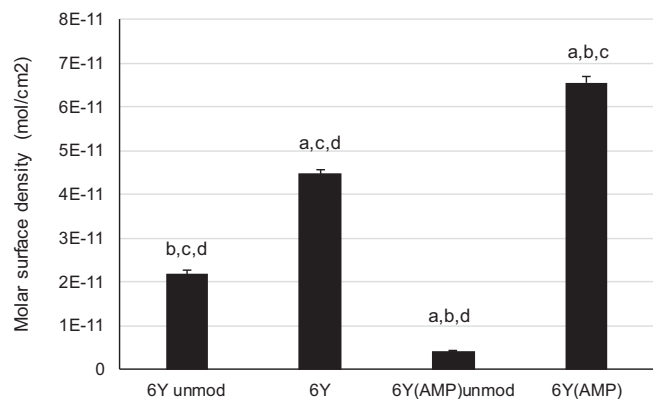


Fig. 3. Molar surface density of 6Y and 6Y(AMP) unmodified and their modified version. Peptides 6Y and 6Y(AMP) showed an increased adhesion in their modified version. The presence of the AMP caused an increased adhesion of the peptide 6Y (AMP) in comparison to peptide 6Y. P value < 0.0001 and multiple comparison revealed significant differences between groups. a, P < 0.0001 compared with 6Yunmod; b, P < 0.0001 compared 6Y; c, P < 0.0001 compared with 6Y(AMP)unmod; d, P < 0.0001 compared with 6Y(AMP).

titanium surface. However, the following antimicrobial assays contradict this hypothesis.

3.3. Antimicrobial assays on substrate

To determine if the proposed coatings could be projected as a protection for titanium orthopedic implants, small substrates made of titanium were coated with peptides 6Y(AMP) and 6Y and the coated and uncoated samples were subjected to a cell culture of *Staphylococcus aureus* and *Staphylococcus epidermidis* in exponential growth phase.

Substrates treated with Live/Dead staining kit (Sigma-Aldrich) are shown in Fig. 5, where live bacteria are visualized as green cells, while dead ones are red (Fig. 5). As can be seen in Fig. 5a and d, the uncoated substrates showed a high density of live bacteria, while both peptides had a potent antifouling activity against *S. aureus*, with less living and dead bacteria observed on the coated surfaces (Fig. 5b and c). However, the coatings seem to have no effect against *S. epidermidis*, since bacteria survival and proliferation appear to be the same with and without the presence of the peptides 6Y(AMP) and 6Y (Fig. 5e and f). Furthermore, even when a lower density of *S. aureus* was observed in substrate coated with peptide 6Y(AMP) (Fig. 5b), its capture could be comparable with 6Y (Fig. 5c), suggesting that the antimicrobial sequence does not contribute to the activity.

The absence of an antimicrobial effect was confirmed by a scanning electron microscopy analysis (Fig. 6), where both bacteria remained intact even on substrates coated with the 6Y(AMP) peptide (Fig. 6b, 6d and 6e). However, according to Live/Dead staining

assays, reduced *S. aureus* proliferation on substrate coated with the bifunctional peptide was observed (Fig. 6b).

To quantify the antifouling effect of both coatings against *Staphylococcus* strains, a detachment protocol of adhered bacteria to coated and uncoated substrates was conducted. The growth kinetics of detached bacteria is shown in Fig. 7a and c for *S. aureus* and *S. epidermidis*, respectively. The bacteria detached from the substrates coated with the 6Y peptide showed a lower initial absorbance (at t_0) than in the case of the bifunctional peptide 6Y (AMP), which suggests a mostly antifouling effect, independent of the presence of the antimicrobial sequence.

Finally, Fig. 7b and d shows the absorbance values at $t_0 = 0$ h and $t_f = 24$ h of growth kinetics for all samples of *S. aureus* and *S. epidermidis*, respectively. Peptides 6Y(AMP) and 6Y prevented the initial *S. aureus* adhesion by 38% and 75.6%, respectively, regardless of the presence of the antimicrobial sequence. A reduction of 45% in *S. epidermidis* adhesion compared to nude substrate was observed, although this difference was not significant. It must be noted that during this kinetic experiment, the bacteria were growing without the presence of the substrate or the coatings, so the difference between absorbance values at $t_f = 24$ h tends to be less obvious.

All these data indicate that, even when the synthesis of pEM-2 together with the adhesive sequence seems not to affect the α -helix structure of the antimicrobial peptide, the adhesion process leads to the loss of its bactericidal activity. This may be due to some minor conformational changes resulting from substrate adhesion, or because some of the Lys residues of the antimicrobial peptide are involved in crosslinking between peptide chains. However, it must be noted that, even without bactericidal effect, peptide 6Y prevents the *S. aureus* by 75.6%.

In a comprehensive study, Ostuni et al. [36] tested the ability of a wide range of self-assembled monolayers to resist protein adsorption, describing the so called “Whitesides rules” that indicate that those monolayers that are hydrophilic, electrically neutral, and containing hydrogen bond acceptors, are more effective in resisting protein adsorption [37]. Although peptide 6Y has a positive net charge, due to the presence of multiple lysine residues, most residues, like DOPA, could be involved in adhesion to titanium and in producing cohesion of the film. In this way, the hydrophilic cover formed by hiding the positively charged residues would avoid interaction with proteins and potentially with microorganisms as well.

This may explain the powerful antifouling effect of peptide 6Y against the *S. aureus* strain. This effect was not so obvious against *S. epidermidis*, according to the results of the live/dead staining, SEM and the detachment protocol. The explanation could be in the proteins involved in the primary adhesion to inert surfaces, like *S. epidermidis* accumulation-associated protein (Aap) and the Bap homologous protein (Bhp).

Bioinformatics analyses suggest that the Aap protein consists in two domains, denoted as A and B [38,39]. This protein and its orthologous, SasG (*S. aureus* surface protein G), have been shown

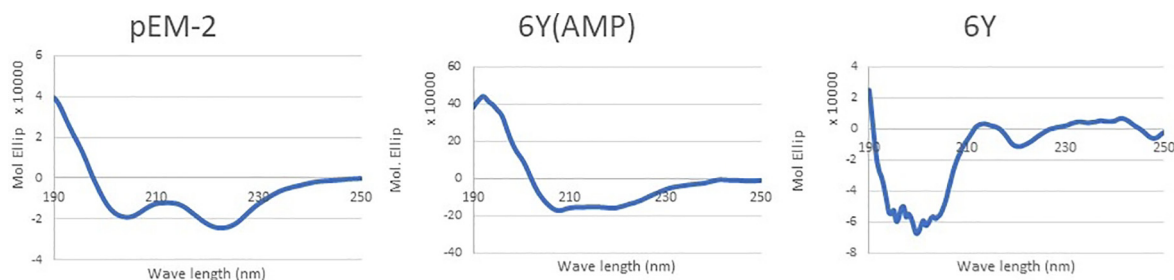


Fig. 4. Circular dichroism analysis of the antimicrobial peptide pEM-2, the bifunctional peptide 6Y(AMP) and the adhesive peptide 6Y. Antimicrobial peptide pEM-2 and bifunctional peptide 6Y(AMP) showed a α -helix structure, while peptide 6Y showed a random structure.

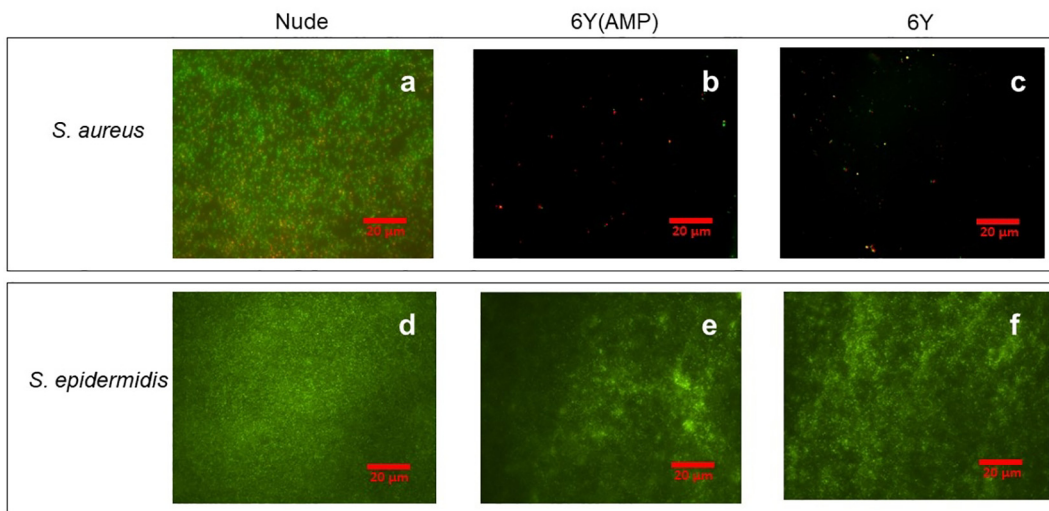


Fig. 5. Fluorescence microscopy images of nude and coated substrate with 6Y(AMP) and 6Y peptides and then treated with *S. aureus* (a, b and c) and *S. epidermidis* (d, e and f) bacteria. Live bacteria are shown in green, dead ones in red.

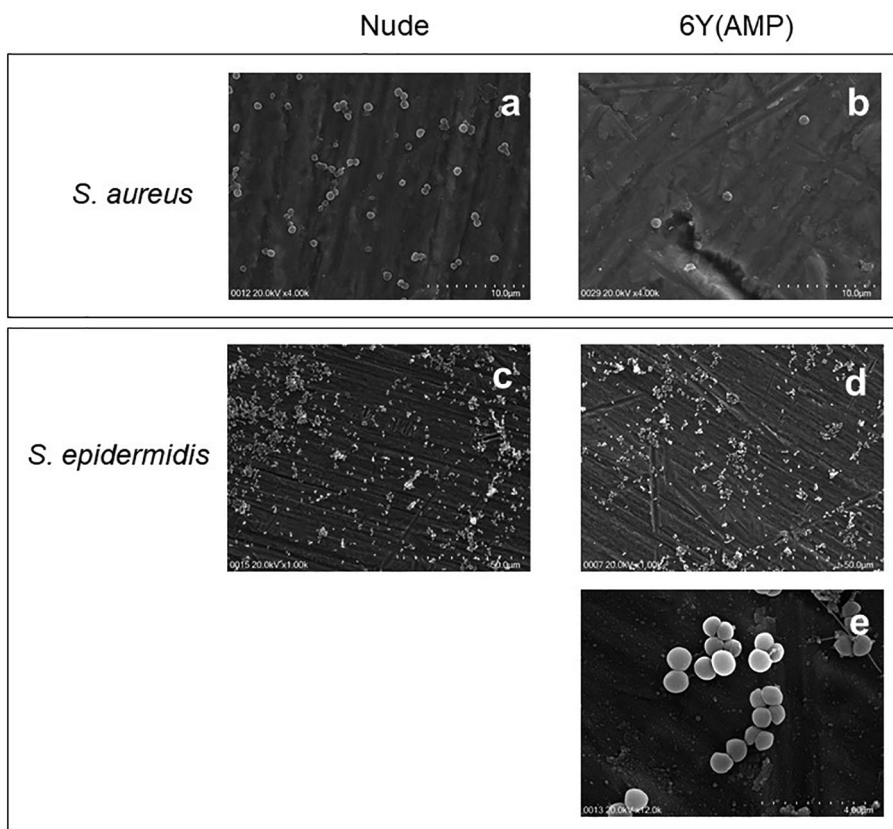


Fig. 6. Scanning electron microscopy images of nude and coated substrates with 6Y(AMP) peptide and then treated with *S. aureus* (a, b) and *S. epidermidis* (c, d and e) bacteria.

to mediate biofilm formation in the absence of PIA (polysaccharide intercellular adhesin). To this purpose, domain A must be cleaved, allowing the dimerization of the B domains with adjacent bacteria, facilitating bacteria accumulation [40]. While the processing of Aap and SasG differs, inhibition of proteolytic cleavage of domain A prevents biofilm formation in both species [41].

On the other hand, Bhp was first posted by Bowden et al. [38] as the *S. aureus* Bap (biofilm-associated protein) homologue from *S. epidermidis* RP62A, which has been proposed as a promoter of

the primary binding of this strain on abiotic surfaces, as well as intercellular adhesion during the formation of biofilms. In contrast to Aap, which is found in approximately 90% of *S. epidermidis* isolates, Bhp is encoded in approximately 15–45% of the isolates [42]. In *S. aureus*, Bap is even less frequent and Vautor et al. [43] found that *bhp* was not encoded in 262 *S. aureus* isolates obtained from various animal and human sources. Bap is mostly present in bovine mastitis isolates of *S. aureus*, and their absence from human clinical isolates is because Bap-mediated biofilm formation seems

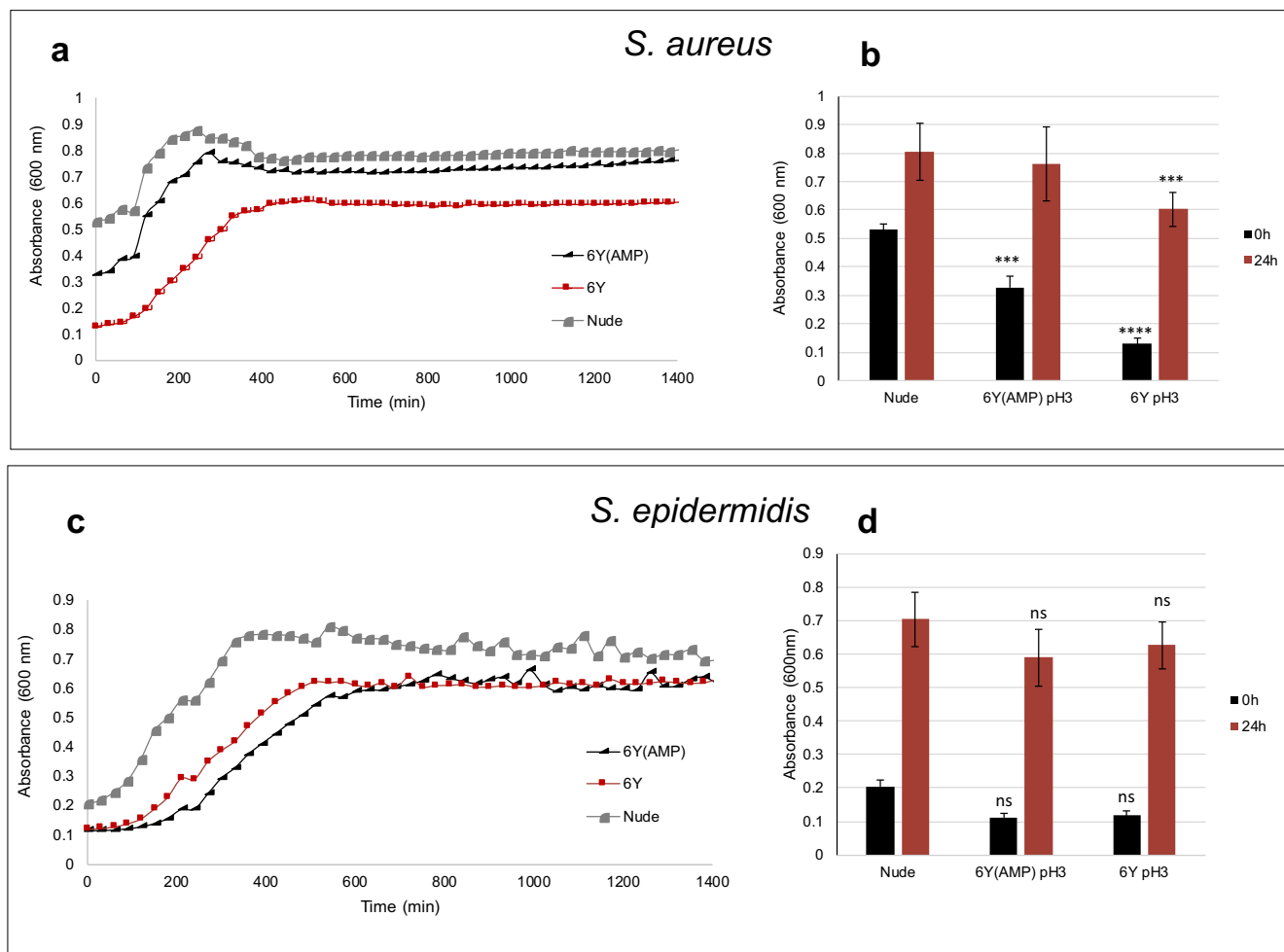


Fig. 7. Growth of (a) *S. aureus* and (c) *S. epidermidis* as a function of time after the detachment protocol. (b and d) Absorbance as a measure of the detached bacteria at $t_0 = 0$ h and $t_f = 24$ h for (b) *S. aureus* and (d) *S. epidermidis*.

to be a system specialized for the conditions present in the mammary gland, where calcium concentration can reach the high values necessary to modulate Bap function (~ 10 mM) [44].

Based on the fact that *S. epidermidis* RP62A strain used in this study (ATCC 35984) contains the *bhp* gen, we wonder if the Bhp protein, is as decisive in its adhesion on titanium surfaces as to hinder the antifouling action of the peptides used in this study. Additional analysis is required to answer this question.

Finally, even when the presence of the antimicrobial peptide does not contribute to the activity, an adhesive peptide with only 13 amino acid residues, derived from the Mfp-5 of *Mytilus edulis* mussel, proved to be enough to show an antifouling effect preventing *S. aureus* and *S. epidermidis* adhesion to titanium surface by 75.6% and 45%, respectively. This result was obtained in the absence of additional chemical groups, like poly(ethylene oxide) or poly(sulfobetaine methacrylate), typically used to obtain antifouling surfaces based on polymer brushes.

4. Conclusions

The reported results demonstrate that a sequence derived from the mussel adhesive protein Mfp-5 can be synthesized with coating effect on titanium surfaces. As expected, the adhesion of this type of coatings is intimately linked to DOPA residues, where Tyr modification is necessary. Interestingly, the presence of the antimicrobial sequence pEM-2 showed to favor the adhesion due to its high content of Lys residues, which may increase the crosslinking

between peptide chains but reduce the antimicrobial activity. Consequently, the bifunctional peptide constructed by the adhesive and the pEM-2 sequences, did not show bactericidal characteristics. However, a powerful antifouling activity was observed, the adhesive sequence by itself being enough to reduce *S. aureus* adhesion by 75%. In conclusion, this 13-res peptide derived from a natural and biocompatible source, like *Mytilus* mussel, could be projected as a possible protective agent against pathogens on titanium surfaces, typically used in orthopedic implants.

Financial support

This work was partially funded by the National Agency for Research and Development (ANID)/Scholarship Program/DOCTOR-ADO BECAS CHILE/2016-21160076 and the Incentive Program for Scientific Initiation (PIIC) of the Universidad Técnica Federico Santa María.

Conflict of interest

The authors declare no conflicts of interest.

Acknowledgments

Special thanks to Dr. Herbert Waite of Marine Science Institute and Department of Molecular Cell and Developmental Biology, University of California, Santa Barbara.

References

- [1] Ribeiro M, Monteiro FJ, Ferraz MP. Infection of orthopedic implants with emphasis on bacterial adhesion process and techniques used in studying bacterial-material interactions. *Biomater* 2012;2(4):176–94. <https://doi.org/10.4161/biom.22905>. PMID: 23507884.
- [2] Arciola CR, Campoccia D, Speziale P, et al. Biofilm formation in *Staphylococcus* implant infections. A review of molecular mechanisms and implications for biofilm-resistant materials. *Biomaterials* 2012;33(26):5967–82. <https://doi.org/10.1016/j.biomaterials.2012.05.031>. PMID: 22695065.
- [3] Kargupta R, Bok S, Darr CM, et al. Coatings and surface modifications imparting antimicrobial activity to orthopedic implants. *Wiley Interdiscip Rev Nanomed Nanobiotechnol* 2014;6(5):475–95. <https://doi.org/10.1002/wnan.1273>. PMID: 24867883.
- [4] Kazemzadeh-Narbat M, Lai BF, Ding C, et al. Multilayered coating on titanium for controlled release of antimicrobial peptides for the prevention of implant-associated infections. *Biomaterials* 2013;34(24):5969–77. <https://doi.org/10.1016/j.biomaterials.2013.04.036>. PMID: 23680363.
- [5] Chen J, Zhu Y, Xiong M, et al. Antimicrobial titanium surface via click-immobilization of peptide and its in vitro/vivo activity. *ACS Biomater Sci Eng* 2019;5(2):1034–44. <https://doi.org/10.1021/acsbomaterials.8b01046>. PMID: 33405794.
- [6] Gao G, Lange D, Hilpert K, et al. The biocompatibility and biofilm resistance of implant coatings based on hydrophilic polymer brushes conjugated with antimicrobial peptides. *Biomaterials* 2011;32(16):3899–909. <https://doi.org/10.1016/j.biomaterials.2011.02.013>. PMID: 21377727.
- [7] Mishra B, Reiling S, Zarena D, et al. Host defense antimicrobial peptides as antibiotics: Design and application strategies. *Curr Opin Chem Biol* 2017;38:87–96. <https://doi.org/10.1016/j.copba.2017.03.014>. PMID: 28399505.
- [8] Ramesh S, Govender T, Kruger HG, et al. Short antimicrobial peptides (SAMPs) as a class of extraordinary promising therapeutic agents. *J Pept Sci* 2016;22(7):438–51. <https://doi.org/10.1002/psc.2894>. PMID: 27352996.
- [9] Haney EF, Mansour SC, Hancock RE. Antimicrobial peptides: An introduction. *Methods Mol Biol* 2017;1548:3–22. https://doi.org/10.1007/978-1-4939-6737-7_1. PMID: 28013493.
- [10] Boparai JK, Sharma PK. Mini review on antimicrobial peptides, sources, mechanism and recent applications. *Protein Pept Lett* 2020;27(1):4–16. <https://doi.org/10.2174/0929866526666190822165812>. PMID: 31438824.
- [11] Marqus S, Pirogova E, Piva TJ. Evaluation of the use of therapeutic peptides for cancer treatment. *J Biomed Sci* 2017;24(1):21. <https://doi.org/10.1186/s12929-017-0328-x>. PMID: 28320393.
- [12] Santamaría C, Larios S, Angulo Y, et al. Antimicrobial activity of myotoxic phospholipase A₂ from crotalid snake venoms and synthetic peptide variants derived from their C-terminal region. *Toxicon* 2005;45(7):807–15. <https://doi.org/10.1016/j.toxicon.2004.09.012>. PMID: 15904676.
- [13] Murillo LA, Lan CY, Agabian NM, et al. Fungicidal activity of a phospholipase-A₂-derived synthetic peptide variant against *Candida albicans*. *Rev Esp Quimioter* 2007;20(3):330–3. PMID: 18080030.
- [14] Nicklisch SC, Waite JH. Mini-review: The role of redox in DOPA-mediated marine adhesion. *Biofouling* 2012;28(8):865–77. <https://doi.org/10.1080/08927014.2012.719023>. PMID: 22924420.
- [15] Lee BP, Messersmith PB, Israelachvili JN, et al. Mussel-inspired adhesives and coatings. *Annu Rev Mater Sci* 2011;41(1):99–132. <https://doi.org/10.1146/annurev-matsci-062910-100429>. PMID: 22058660.
- [16] Waite JH. Mussel adhesion - essential footwork. *J Exp Biol* 2017;220(4):517–30. <https://doi.org/10.1242/jeb.134056>. PMID: 28202646.
- [17] Kuang J, Messersmith PB. Universal surface-initiated polymerization of antifouling zwitterionic brushes using a mussel-mimetic peptide initiator. *Langmuir* 2012;28(18):7258–66. <https://doi.org/10.1021/ja300738e>. PMID: 22506651.
- [18] Wilke P, Börner H. Mussel-glycine derived peptide-polymer conjugates to realize enzyme-activated ml coatings. *ACS Macro Lett* 2012;1:871–5. <https://doi.org/10.1021/mz300258m>.
- [19] Mu Y, Wu Z, Pei D, et al. A versatile platform to achieve mechanically robust mussel-inspired antifouling coatings via grafting-to approach. *J Mater Chem B* 2018;6(1):133–42. <https://doi.org/10.1039/C7TB02400B>. PMID: 32254201.
- [20] Jo YK, Seo JH, Choi BH, et al. Surface-independent antibacterial coating using silver nanoparticle-generating engineered mussel glue. *ACS Appl Mater Interfaces* 2014;6(22):20242–53. <https://doi.org/10.1021/am505784k>. PMID: 25311392.
- [21] Jo YK, Choi BH, Zhou C, et al. Bioengineered mussel glue incorporated with a cell recognition motif as an osteostimulating bone adhesive for titanium implants. *J Mater Chem B* 2015;3(41):8102–14. <https://doi.org/10.1039/C5TB01230A>. PMID: 32262867.
- [22] Guzmán F, Gauna A, Luna O, et al. The tea-bag protocol for comparison of Fmoc removal reagents in solid-phase peptide synthesis. *Amino Acids* 2020;52(8):1201–5. <https://doi.org/10.1007/s00726-020-02883-8>. PMID: 32851463.
- [23] Guzmán F, Gauna A, Roman T, et al. Tea bags for Fmoc solid-phase peptide synthesis: An example of circular economy. *Molecules* 2021;26(16):5035. <https://doi.org/10.3390/molecules26165035>. PMID: 34443624.
- [24] Wei W, Yu J, Gebbie MA, et al. Bridging adhesion of mussel-inspired peptides: Role of charge, chain length, and surface type. *Langmuir* 2015;31(3):1105–12. <https://doi.org/10.1021/la504316g>. PMID: 25540823.
- [25] Tan Y, Yildiz UH, Wei W, et al. Layer-by-layer polyelectrolyte deposition: A mechanism for forming biocomposite materials. *Biomacromolecules* 2013;14(6):1715–26. <https://doi.org/10.1021/bm400448w>. PMID: 23600626.
- [26] Guzmán F, Wong G, Román T, et al. Identification of antimicrobial peptides from the microalgae *Tetraselmis suecica* (Kylin) butcher and bactericidal activity improvement. *Mar Drugs* 2019;17(8):453. <https://doi.org/10.3390/md17080453>. PMID: 31374937.
- [27] Alvarez CA, Guzmán F, Cárdenas C, et al. Antimicrobial activity of trout hepcidin. *Fish Shellfish Immunol* 2014;41(1):93–101. <https://doi.org/10.1016/j.fsi.2014.04.013>. PMID: 24794583.
- [28] Corrales-Ureña YR, Souza-Schiaber Z, Lisboa-Filho PN, et al. Functionalization of hydrophobic surfaces with antimicrobial peptides immobilized on a bio-interfacial layer. *RSC Adv* 2020;10(1):376–86. <https://doi.org/10.1039/C9RA07380A>.
- [29] Álvarez C, Barriga A, Albericio F, et al. Identification of peptides in flowers of *Sambucus nigra* with antimicrobial activity against aquaculture pathogens. *Molecules* 2018;23(5):1033. <https://doi.org/10.3390/molecules23051033>. PMID: 29702623.
- [30] Kubiak K, Adamczyk Z, Oćwieja M. Kinetics of silver nanoparticle deposition at PAH monolayers: Reference QCM results. *Langmuir* 2015;31(10):2988–96. <https://doi.org/10.1021/la504975z>. PMID: 25692665.
- [31] Li Y, Liang C, Gao L, et al. Hidden complexity of synergistic roles of DOPA and lysine for strong wet adhesion. *Mater Chem Front* 2017;1(12):2664–8. <https://doi.org/10.1039/C7OM00402H>.
- [32] Maier GP, Rapp MV, Waite JH, et al. Adaptive synergy between catechol and lysine promotes wet adhesion by surface salt displacement. *Science* 2015;349(6248):628–32. <https://doi.org/10.1126/science.1260556>. PMID: 26250681.
- [33] Rapp MV, Maier GP, Dobbs HA, et al. Defining the catechol-cation synergy for enhanced wet adhesion to mineral surfaces. *J Am Chem Soc* 2016;138(29):9013–6. <https://doi.org/10.1021/jacs.6b03453>. PMID: 27415839.
- [34] Degen GD, Stow PR, Lewis RB, et al. Impact of molecular architecture and adsorption density on adhesion of mussel-inspired surface primers with catechol-cation synergy. *J Am Chem Soc* 2019;141(47):18673–81. <https://doi.org/10.1021/jacs.9b04337>. PMID: 31771333.
- [35] Yu HY, Yip BS, Tu CH, et al. Correlations between membrane immersion depth, orientation, and salt-resistance of tryptophan-rich antimicrobial peptides. *Biochim Biophys Acta* 2013;1828(11):2720–8. <https://doi.org/10.1016/j.bbame.2013.07.020>. PMID: 23896553.
- [36] Ostuni E, Chapman RG, Holmlin RE, et al. A survey of structure-property relationships of surfaces that resist the adsorption of protein. *Langmuir* 2001;17(18):5605–20. <https://doi.org/10.1021/ja010384m>.
- [37] Le TC, Penna M, Winkler DA, et al. Quantitative design rules for protein-resistant surface coatings using machine learning. *Sci Rep* 2019;9(1). <https://doi.org/10.1038/s41598-018-36597-5>. PMID: 30670792.
- [38] Bowden MG, Chen W, Singvall J, et al. Identification and preliminary characterization of cell-wall-anchored proteins of *Staphylococcus epidermidis*. *Microbiology* 2005;151(5):1453–64. <https://doi.org/10.1099/mic.0.27534-0>. PMID: 15870455.
- [39] Roche FM, Massey R, Peacock SJ, et al. Characterization of novel LPXTG-containing proteins of *Staphylococcus aureus* identified from genome sequences. *Microbiology* 2003;149(3):643–54. <https://doi.org/10.1099/mic.0.25996-0>. PMID: 12634333.
- [40] Conrady DG, Wilson JJ, Herr AB. Structural basis for Zn²⁺-dependent intercellular adhesion in staphylococcal biofilms. *Proc Natl Acad Sci USA* 2013;110(3):E202–11. <https://doi.org/10.1073/pnas.1208134110>. PMID: 23277549.
- [41] Schaeffer CR, Woods KM, Longo GM, et al. Accumulation-associated protein enhances *Staphylococcus epidermidis* biofilm formation under dynamic conditions and is required for infection in a rat catheter model. *Infect Immun* 2015;83(1):214–26. <https://doi.org/10.1128/IAI.02177-14>. PMID: 25332125.
- [42] Fey PD, Olson ME. Current concepts in biofilm formation of *Staphylococcus epidermidis*. *Future Microbiol* 2010;5(6):917–33. <https://doi.org/10.2217/fmb.10.56>. PMID: 20521936.
- [43] Vautor E, Abadie G, Pont A, et al. Evaluation of the presence of the bap gene in *Staphylococcus aureus* isolates recovered from human and animals species. *Vet Microbiol* 2008;127(3–4):407–11. <https://doi.org/10.1016/j.vetmic.2007.08.018>. PMID: 17881161.
- [44] Valle J, Fang X, Lasa I. Revisiting Bap multidomain protein: More than sticking bacteria together. *Front Microbiol* 2020;11. <https://doi.org/10.3389/fmicb.2020.613581>.